Umbrella-like helical structure of alpha-synuclein at the air-water interface observed with experimental and theoretical sum frequency generation spectroscopy.

Kris Strunge,[1] Tucker Burgin,[2] Thaddeus W. Golbek,[1] Steven J. Roeters,[1] Jim Pfaendtner,[2] and Tobias Weidner[1,2,*]

[1] Department of Chemistry, Aarhus University, Langelandsgade 140, 8000 Aarhus C, Denmark

[2] Department of Chemical Engineering, University of Washington, Benson Hall 1750, Seattle, WA 98195-1750, USA

KEYWORDS Interfacial proteins, Parkinson's disease, molecular dynamics simulations, surface spectroscopy, sum frequency generation spectroscopy

ABSTRACT: The misfolding of α-synuclein (aS) into amyloid aggregates is associated with severe brain disorders. Aggregated copies of aS are found in the amyloid aggregates observed in brain tissues from Parkinson's patients. Surfaces are known to catalyze the formation of amyloid aS aggregates. Despite the importance of the role of interfaces and several decades of structural studies, the 3D structure of aS when bound to interfaces is still not completely clear. Hydrophobic interfaces are particularly important here. We report interface-specific sum-frequency generation (SFG) experiments to determine how monomeric aS binds to the air-water interface, a model system for hydrophobic surfaces in general. We model the SFG data by combining the experimental data directly to theoretical spectra calculations from molecular dynamics simulations. We find that aS, which is an intrinsically disordered protein in solution, folds into a defined, mostly helical, secondary structure at the air-water interface. The binding pose is reminiscent of an umbrella-shape, where the C-terminus represents the 'pole' and protrudes into the water phase, while the N-terminus and the NAC region span the canopy at the interface. In this binding pose, aS is prone to aggregate, which could explain the catalytic effect of hydrophobic interfaces and air bubbles on aS fibrillation.

α-Synuclein (αS) is an intrinsically disordered protein with no discernible and stable secondary structure in solution.[1] Interfaces can catalyse the folding of aS and can stabilise a secondary and tertiary structure.[2,3] Misfolding and aggregation into oligomers and fibrils at such interfaces has been associated with serious neurological diseases such as Parkinson's disease.[4–7] Understanding the molecular details of the interaction of aS with surfaces will be an important step towards finding a cure and treatment. The folding of aS at lipid interfaces has been studied with various methods, such as nuclear magnetic resonance (NMR)[8–13], electron paramagnetic resonance (EPR)[8,11], neutron reflectometry[14] and SFG[15–17]. The results draw a picture of effective catalysis of aS into oligomers and fibrils at lipid surfaces.

Hydrophobic interfaces are another type of interface that is omnipresent in biology. Furthermore, in bio-lab settings when handling aS in reaction and storage containers, tubes and sample cells there are many hydrophobic surfaces involved. In addition, the air water interface (AWI), a model hydrophobic interface, plays an important role for the interaction of aS with solvated air bubbles in the sample solution and in vivo.[18,19] A limited number of studies have explored the potential importance of aS aggregation at the AWI using NMR,[20] infrared reflection absorption spectroscopy (IRRAS),[21,22] atomic force microscopy (AFM),[23,24] and fluorescence microscopy[25] but with limited structural resolution. The lack of information about the interfacial folding of aS is likely explained by the limited number of methods available to observe the structure of interfacial proteins in the presence of many more proteins

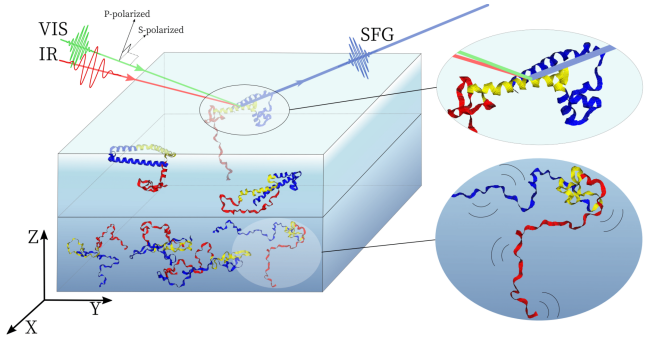

Figure 1. The lab frame SFG geometry of the measurement of α-synuclein at the air-water interface.

in solution. SFG spectroscopy has been developed into a reliable tool to do just that - probe proteins at interfaces.[26–28] The method is based on mixing infrared and visible laser pulses at the interface to obtain a vibrational spectrum. Since SFG is a second order nonlinear process, the signal is exclusively generated at the interface and only bound and ordered proteins will contribute to the signal. SFG is a coherent method and therefore signal coming from different locations within a protein structure can interfere in complex ways.[28] This can lead to the challenge that spectra cannot be analysed by inspection, fitting and direct peak assignment. We have recently developed a suite of computational methods to extract structural information from SFG amide-I spectra by modelling experimental SFG data with theoretical spectra calculated from molecular dynamics (MD) simulations. Here, we use the VISCA-select package to determine how monomeric αS binds, folds, and orients at the AWI.

Figure 1 displays the geometry of the setup used in the SFG experiments. A 3.9 mL Teflon trough is filled with PBS buffer solution after which 0.40 mL of a 200 µM aS solution is injected into the subphase. The solution was prepared using D_2O to avoid spectral overlap of the amide-I region with the water bending mode. The resulting concentration was 19 µM, a concentration close to the physiological value of 22 µM observed in the synapses of rats.[29] aS was allowed to bind and assemble at the interface for 20 min before the first spectra were collected.

Figure 2A shows an overview of spectra recorded in the ssp (s-polarized SFG, s-polarized visible and p-polarized infrared), ppp, sps and psp polarization combinations. The ssp and ppp spectra show a dominant feature near 1645 cm^{-1}. In ssp, a broad double peak is visible with resonances near 1630 cm^{-1} and 1645 cm^{-1}. No significant signal was observed above the noise level for the psp combination. The selection rules of SFG dictate that only molecular layers with a degree of order are visible in the spectra. Disordered and highly dynamic protein structures would not generate discernible SFG peaks. The fact that these spectra are generated at the AWI directly shows that aS binds the interface and assumes an ordered structure unlike what has been reported for aS in solution[29,30]. The data show that aS becomes ordered when interacting with the hydrophobic AWI.

To gain insight into details of the structure of aS in its interfacial state, we compared the experimental data with theoretical spectra using the frame-selection method. We first ran MD simulations to create a large number of hypothetical structures. Then, we used spectra calculations to determine, which frames in the simulation match the experimental data best. In this way, it is possible to determine the surface structure without the need for computationally expensive equilibrium simulations. The simulation were run until an ensemble of well matching structures were found.

MD simulations were performed using GROMACS version 2021.4 [31–39] with the a99SB-disp force field [40]. Details about the MD simulations can be found in the supporting information document. Five copies of α-synuclein crystal structures (from PDB ID: 2KKW[11]) were arranged into a cross shape with their hydrophobic surfaces facing the same direction. The system was solvated such that their hydrophobic surfaces were flush with the edge of the box. Six independent simulations were run in the NVT ensemble at 300 K for roughly 100 ns each. The vacuum-water interface was observed to be stable over the course of the simulations, and in each independent simulation at least five of the six proteins remained at the interface for the entire simulation runtime.

Spectral calculations were performed on the MD sampled α-synuclein structures using the excitonic Hamiltonian approach to frequency mapping developed previously.[26,41] The model maps the protein structure and orientation to the SFG spectrum in the amide-I region by constructing an excitonic Hamiltonian.

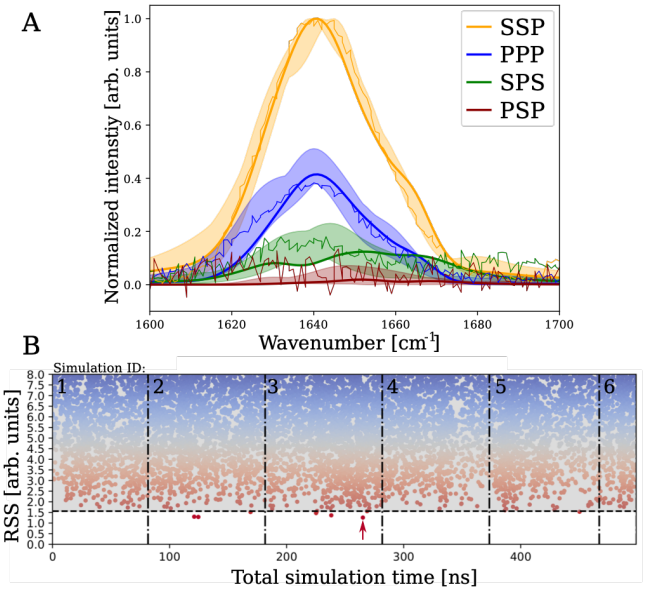

Figure 2. (A) Experimental SFG spectrum (thin line) of α-synuclein at the air-water interface in the amide-I region, the simulated SFG spectrum (thick line) of structure "A" corresponding to the lowest residual sum-of-squares (RSS). The shaded area marks the upper and lower bounds of the simulated spectra from the best matching ensemble. (A) The RSS estimating the deviation between simulated and experimental

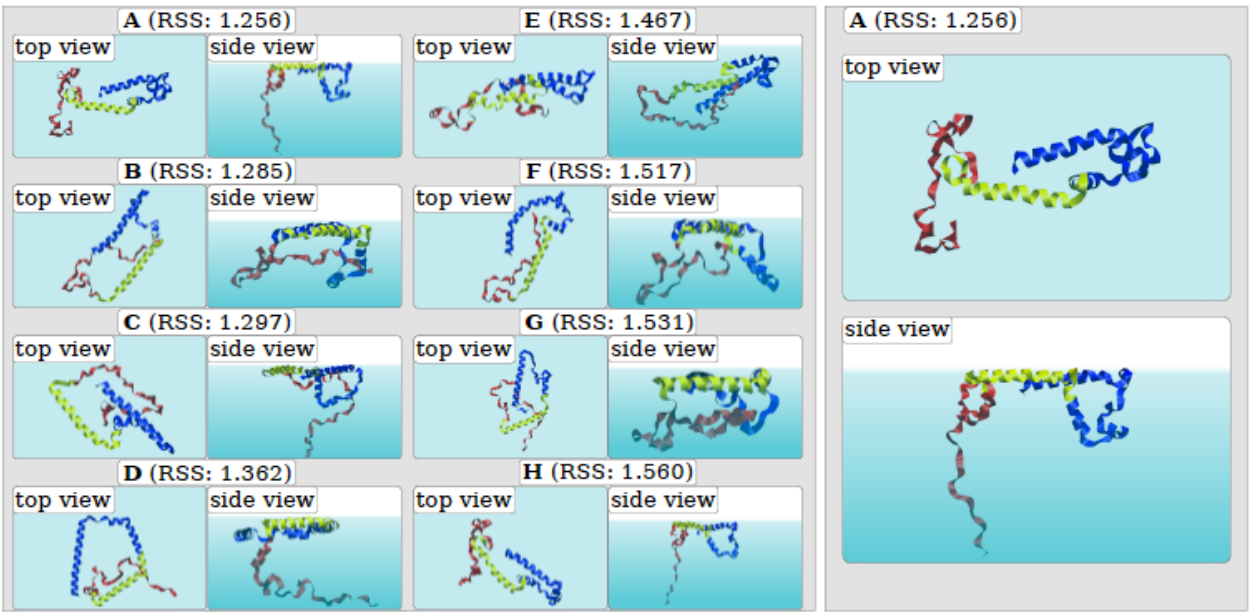

Figure 3. The best matching ensemble of structures identified by the RSS below 1.561. The general structural motif is identified by two α-helices in the N-terminal (blue) and NAC region (yellow) respectively with both lying parallel to the interface. A small amount of α-helix is found to orient perpendicular to the interface. The C-terminal region (red) is disordered and stays solvated.

spectra for each frame in the six MD simulations. The RSS cut-off value (dashed horizontal line) is chosen such that the standard variation in the simulated spectra matches the standard variation in the series of experimental spectra. It results in a best matching ensemble consisting of 8 protein structures with RSS below the cutoff 1.561 whereof the best matching structure "A" is marked with a red arrow.

The construction combines structural parameters and physical parameters such as the C=O bond lengths, orientations and distances to calculate the local mode frequencies including hydrogen bond shifts[42,43] and couplings between the local modes[44–46] (see SI for more details).

The match between experimental and calculated SFG spectra was evaluated for each structure from the combined 500 ns of MD simulations by calculating the residual sum-of-squares (RSS) value. Figure 2B shows the RSS values for all frames of the simulations. The spectral shape and polarization ratios are highly dependent on the orientation and conformation as evident by the highly fluctuating RSS values shown in Figure 2B. This shows SFG spectra have potential to discriminate between different structural states. This is an advantage of such a SFG spectral analysis, which has previously been observed for other proteins.[26,47,48]

Even though aS is proposed to obtain more structure when interacting with hydrophobic interfaces[11,21], it is expected to retain a high degree of flexibility. To embrace this in the simulations we generated an ensemble of the matching structures instead of focusing on a single best matching pose. The size of the ensemble was determined such that the variance in the modelled spectra was equal to the variance in the series of experimental spectra. We define a RSS cut-off, for which the ensemble of structures with RSS values below the cut-off have a spectral standard variation in the simulated spectra that matches the standard variation in the series of experimental spectra. Based on this criterium, the cut-off RSS value in our analysis was 1.561. The cut-off is indicated in Figure 2B as a horizontal line. We obtained a matching ensemble consisting of 8 protein structures with an RSS value below the RSS cut-off value (See Figure 3).

The ensemble shows that aS is somewhat flexible at the interface but also that the matching structures have several structural features in common. It is reassuring that the frame selection method is selecting snapshots with common structural features. All snapshots clearly show that aS undergoes a structural transition from the previously-reported disordered state in solution to a folded state when interacting with the hydrophobic interface.

For a closer look at the interfacial folding, it is instructive to examine the different domains of aS. The N-terminal domain (blue) is thought to anchor aS to membrane surfaces and help stabilize interfacial folding.[10,12] The non-amyloid-β component (NAC, labeled yellow) of aS is the region which has been identified as the main driver of amyloid aggregation and fibril formation.[49] The C-terminal domain (red) is typically very mobile even in aS oligomers, and is thought to remain unbound at membrane surfaces and available to bind to presynaptic vesicles. At the AWI, all snapshots show that both the N-terminus and the NAC region bind the surface in a helical fold with the long helix axis parallel to the surface. As can be seen in the side views if the snapshot plots, in this conformation, the C-terminal domain remains unbound and unfolded and protrudes into the aqueous phase. The only exception here is struc-

ture "E", where the C-terminus is located in moderate proximity to the surface. However, even in this geometry the C-terminus remains unfolded, indicating limited interaction with the AWI.

Figure 3B highlights the general folding motif for the best-matching structure "A". The spectral calculations on Figure 2A show a very good match of the relative intensities of the different polarization combinations. For ssp and ppp, the spectra shapes are captured well by the simulations. The spectra shape of the modes in sps polarization is shifted by ca. 15 cm^{-1}. It should be noted that the overall spectral signal to noise ratio is also highest for the three non-chiral contributions. The chiral psp combination yields no signal in experiment and simulations, which is expected for amide-I SFG of α-helical structures.[28]

For structure "A", the N-terminal and NAC regions fold into helices at the interface. While both domains together assume a U-shape at the surface, the C-terminus is not attached to the interface and is protruding into the bulk phase. The C-terminus is fully solvated and remains largely unstructured. Together, the three domains form an umbrella-like tertiary structure, where the N-terminus and the NAC region span a canopy and the C-terminus represents the pole. This umbrella structure motif is repeated in almost all structures in the best matching ensemble.

The exposure of the aggregation-prone NAC-region at the interface in a folded state likely promotes oligomerization within the aS layer, because the NAC regions are brought in close proximity. An α-helical secondary structure has often been observed as an early intermediate structure in αS aggregation.[50,51] The umbrella structure can explain the induction of aS aggregation by hydrophobic interfaces and air contacts in particular. It could also provide an explanation for accelerated fibril formation by shaking of aS solutions. Shaking is a central method in aS research to obtain fibrils and oligomers within reasonable time frames, but at the molecular level, the process is still debated. It is clear that shaking of protein solutions creates microscopic air bubbles.[18,19] In view of the binding geometry at the AWI, binding of aS to the interfaces of microscopic air bubbles in solution will promote aggregation and, consequently, fibrillation.

ASSOCIATED CONTENT

Supporting Information

The Supporting Information is available free of charge on the ACS Publications website.

brief description (file type, i.e., PDF)

brief description (file type, i.e., PDF)

AUTHOR INFORMATION

Corresponding Author

* Tobias Weidner: weidner@chem.au.dk

ACKNOWLEDGMENT

The authors acknowledge Prof. Daniel Otzen from the Interdisciplinary Nanoscience Centre (iNANO), Aarhus University, for generously providing the αS samples. This article is part of a project that has received funding from the European Research Council (ERC) under the European Union's Horizon 2020 research and innovation program (Grant Agreement No. 819039 F-BioIce). SJR acknowledges the Lundbeck Foundation for funding through the post-doctoral award R303-2018-349. TWG thanks the Lundbeck Foundation for a postdoc fellowship (postdoc grant R322-2019-2461).

REFERENCES

(1) Grupi, A.; Haas, E. Segmental Conformational Disorder and Dynamics in the Intrinsically Disordered Protein α-Synuclein and Its Chain Length Dependence. *J. Mol. Biol.* **2011**, *405* (5), 1267–1283. https://doi.org/10.1016/j.jmb.2010.11.011.

(2) Ruipérez, V.; Darios, F.; Davletov, B. Alpha-Synuclein, Lipids and Parkinson's Disease. *Prog. Lipid Res.* **2010**, *49* (4), 420–428. https://doi.org/10.1016/j.plipres.2010.05.004.

(3) Iyer, A.; Claessens, M. M. A. E. Disruptive Membrane Interactions of Alpha-Synuclein Aggregates. *Biochim. Biophys. Acta BBA - Proteins Proteomics* **2019**, *1867* (5), 468–482. https://doi.org/10.1016/j.bbapap.2018.10.006.

(4) Breydo, L.; Wu, J. W.; Uversky, V. N. α-Synuclein Misfolding and Parkinson's Disease. *Biochim. Biophys. Acta BBA - Mol. Basis Dis.* **2012**, *1822* (2), 261–285. https://doi.org/10.1016/j.bbadis.2011.10.002.

(5) Wong, Y. C.; Krainc, D. α-Synuclein Toxicity in Neurodegeneration: Mechanism and Therapeutic Strategies. *Nat. Med.* **2017**, *23* (2), 1–13. https://doi.org/10.1038/nm.4269.

(6) Singh, S. K.; Dutta, A.; Modi, G. α-Synuclein Aggregation Modulation: An Emerging Approach for the Treatment of Parkinson's Disease. *Future Med. Chem.* **2017**, *9* (10), 1039–1053. https://doi.org/10.4155/fmc-2017-0016.

(7) Alafuzoff, I.; Hartikainen, P. Chapter 24 - Alpha-Synucleinopathies. In *Handbook of Clinical Neurology*; Kovacs, G. G., Alafuzoff, I., Eds.; Neuropathology; Elsevier, 2018; Vol. 145, pp 339–353. https://doi.org/10.1016/B978-0-12-802395-2.00024-9.

(8) Ulmer, T. S.; Bax, A.; Cole, N. B.; Nussbaum, R. L. Structure and Dynamics of Micelle-Bound Human α-Synuclein*. *J. Biol. Chem.* **2005**, *280* (10), 9595–9603. https://doi.org/10.1074/jbc.M411805200.

(9) Georgieva, E. R.; Ramlall, T. F.; Borbat, P. P.; Freed, J. H.; Eliezer, D. Membrane-Bound α-Synuclein Forms an Extended Helix: Long-Distance Pulsed ESR Measurements Using Vesicles, Bicelles, and Rodlike Micelles. *J. Am. Chem. Soc.* **2008**, *130* (39), 12856–12857. https://doi.org/10.1021/ja804517m.

(10) Bodner, C. R.; Dobson, C. M.; Bax, A. Multiple Tight Phospholipid-Binding Modes of α-Synuclein Revealed by Solution NMR Spectroscopy. *J. Mol. Biol.* **2009**, *390* (4), 775–790. https://doi.org/10.1016/j.jmb.2009.05.066.

(11) Rao, J. N.; Jao, C. C.; Hegde, B. G.; Langen, R.; Ulmer, T. S. A Combinatorial NMR and EPR Approach for Evaluating the Structural Ensemble of Partially Folded Proteins. *J. Am. Chem. Soc.* **2010**, *132* (25), 8657–8668. https://doi.org/10.1021/ja100646t.

(12) Fusco, G.; De Simone, A.; Gopinath, T.; Vostrikov, V.; Vendruscolo, M.; Dobson, C. M.; Veglia, G. Direct Observation of the Three Regions in α-Synuclein That Determine Its Membrane-Bound Behaviour. *Nat. Commun.* **2014**, *5* (1), 1–8. https://doi.org/10.1038/ncomms4827.

(13) Antonschmidt, L.; Dervişoğlu, R.; Sant, V.; Tekwani Movellan, K.; Mey, I.; Riedel, D.; Steinem, C.; Becker, S.; Andreas, L. B.; Griesinger, C. Insights into the Molecular Mechanism of

Amyloid Filament Formation: Segmental Folding of α-Synuclein on Lipid Membranes. *Sci. Adv.* **2021**, *7* (20), eabg2174. https://doi.org/10.1126/sciadv.abg2174.

(14) Hellstrand, E.; Grey, M.; Ainalem, M.-L.; Ankner, J.; Forsyth, V. T.; Fragneto, G.; Haertlein, M.; Dauvergne, M.-T.; Nilsson, H.; Brundin, P.; Linse, S.; Nylander, T.; Sparr, E. Adsorption of α-Synuclein to Supported Lipid Bilayers: Positioning and Role of Electrostatics. *ACS Chem. Neurosci.* **2013**, *4* (10), 1339–1351. https://doi.org/10.1021/cn400066t.

(15) Ma, G.; Liu, J.; Fu, L.; Yan, E. C. Y. Probing Water and Biomolecules at the Air–Water Interface with a Broad Bandwidth Vibrational Sum Frequency Generation Spectrometer from 3800 to 900 Cm^{-1}. *Appl. Spectrosc.* **2009**, *63* (5), 528–537.

(16) Sarkar, S.; Bisoi, A.; Singh, P. C. Understanding of the Interaction of Biological Macromolecules with Lipids Using Vibrational Sum-Frequency Generation Spectroscopy. *J. Raman Spectrosc.* **2022**, *53* (10), 1828–1837. https://doi.org/10.1002/jrs.6429.

(17) Biswas, B.; Roy, S.; Mondal, J. A.; Singh, P. C. Interaction of α-Synuclein with Phospholipids and the Associated Restructuring of Interfacial Lipid Water: An Interface-Selective Vibrational Spectroscopic Study. *Angew. Chem.* **2020**, *132* (50), 22919–22925. https://doi.org/10.1002/ange.202011179.

(18) Polinski, N. K.; Volpicelli-Daley, L. A.; Sortwell, C. E.; Luk, K. C.; Cremades, N.; Gottler, L. M.; Froula, J.; Duffy, M. F.; Lee, V. M. Y.; Martinez, T. N.; Dave, K. D. Best Practices for Generating and Using Alpha-Synuclein Pre-Formed Fibrils to Model Parkinson's Disease in Rodents. *J. Park. Dis.* **2018**, *8* (2), 303–322. https://doi.org/10.3233/JPD-171248.

(19) Giehm, L.; Lorenzen, N.; Otzen, D. E. Assays for α-Synuclein Aggregation. *Methods* **2011**, *53* (3), 295–305. https://doi.org/10.1016/j.ymeth.2010.12.008.

(20) Chaari, A.; Horchani, H.; Frikha, F.; Verger, R.; Gargouri, Y.; Ladjimi, M. Surface Behavior of α-Synuclein and Its Interaction with Phospholipids Using the Langmuir Monolayer Technique: A Comparison between Monomeric and Fibrillar α-Synuclein. *Int. J. Biol. Macromol.* **2013**, *58*, 190–198. https://doi.org/10.1016/j.ijbiomac.2013.03.057.

(21) Wang, C.; Shah, N.; Thakur, G.; Zhou, F.; Leblanc, R. M. α-Synuclein in α-Helical Conformation at Air–Water Interface: Implication of Conformation and Orientation Changes during Its Accumulation/Aggregation. *Chem. Commun.* **2010**, *46* (36), 6702–6704. https://doi.org/10.1039/CoCC02098B.

(22) Wang, C.; Sharma, S. K.; Olaluwoye, O. S.; Alrashdi, S. A.; Hasegawa, T.; Leblanc, R. M. Conformation Change of α-Synuclein(61—95) at the Air-Water Interface and Quantitative Measurement of the Tilt Angle of the Axis of Its α-Helix by Multiple Angle Incidence Resolution Spectroscopy. *Colloids Surf. B Biointerfaces* **2019**, *183*, 110401. https://doi.org/10.1016/j.colsurfb.2019.110401.

(23) Zhou, J.; Ruggeri, F. S.; Zimmermann, M. R.; Meisl, G.; Longo, G.; Sekatskii, S. K.; Knowles, T. P. J.; Dietler, G. Effects of Sedimentation, Microgravity, Hydrodynamic Mixing and Air–Water Interface on α-Synuclein Amyloid Formation. *Chem. Sci.* **2020**, *11* (14), 3687–3693. https://doi.org/10.1039/D0SC00281J.

(24) Buell, A. K.; Galvagnion, C.; Gaspar, R.; Sparr, E.; Vendruscolo, M.; Knowles, T. P. J.; Linse, S.; Dobson, C. M. Solution Conditions Determine the Relative Importance of Nucleation and Growth Processes in α-Synuclein Aggregation. *Proc. Natl. Acad. Sci.* **2014**, *111* (21), 7671–7676. https://doi.org/10.1073/pnas.1315346111.

(25) Campioni, S.; Bagnani, M.; Pinotsi, D.; Lecinski, S.; Rodighiero, S.; Adamcik, J.; Mezzenga, R. Interfaces Determine the Fate of Seeded α-Synuclein Aggregation. *Adv. Mater. Interfaces* **2020**, *7* (11), 2000446. https://doi.org/10.1002/admi.202000446.

(26) Hosseinpour, S.; Roeters, S. J.; Bonn, M.; Peukert, W.; Woutersen, S.; Weidner, T. Structure and Dynamics of Interfacial Peptides and Proteins from Vibrational Sum-Frequency Generation Spectroscopy. *Chem. Rev.* **2020**, *120* (7), 3420–3465. https://doi.org/10.1021/acs.chemrev.9b00410.

(27) Ye, S.; Nguyen, K. T.; Clair, S. V. L.; Chen, Z. In Situ Molecular Level Studies on Membrane Related Peptides and Proteins in Real Time Using Sum Frequency Generation Vibrational Spectroscopy. *J. Struct. Biol.* **2009**, *168* (1), 61–77. https://doi.org/10.1016/j.jsb.2009.03.006.

(28) Fu, L.; Wang, Z.; Yan, E. C. Y. Chiral Vibrational Structures of Proteins at Interfaces Probed by Sum Frequency Generation Spectroscopy. *Int. J. Mol. Sci.* **2011**, *12* (12), 9404–9425. https://doi.org/10.3390/ijms12129404.

(29) Wilhelm, B. G.; Mandad, S.; Truckenbrodt, S.; Kröhnert, K.; Schäfer, C.; Rammner, B.; Koo, S. J.; Claßen, G. A.; Krauss, M.; Haucke, V.; Urlaub, H.; Rizzoli, S. O. Composition of Isolated Synaptic Boutons Reveals the Amounts of Vesicle Trafficking Proteins. *Science* **2014**, *344* (6187), 1023–1028. https://doi.org/10.1126/science.1252884.

(30) Robustelli, P.; Piana, S.; Shaw, D. E. Developing a Molecular Dynamics Force Field for Both Folded and Disordered Protein States. *Proc. Natl. Acad. Sci.* **2018**, *115* (21), E4758–E4766. https://doi.org/10.1073/pnas.1800690115.

(31) Hess, B.; Kutzner, C.; van der Spoel, D.; Lindahl, E. GROMACS 4: Algorithms for Highly Efficient, Load-Balanced, and Scalable Molecular Simulation. *J. Chem. Theory Comput.* **2008**, *4* (3), 435–447. https://doi.org/10.1021/ct7003301q.

(32) Van Der Spoel, D.; Lindahl, E.; Hess, B.; Groenhof, G.; Mark, A. E.; Berendsen, H. J. C. GROMACS: Fast, Flexible, and Free. *J. Comput. Chem.* **2005**, *26* (16), 1701–1718. https://doi.org/10.1002/jcc.20291.

(33) Lindahl, E.; Hess, B.; van der Spoel, D. GROMACS 3.0: A Package for Molecular Simulation and Trajectory Analysis. *Mol. Model. Annu.* **2001**, *7* (8), 306–317. https://doi.org/10.1007/s008940100045.

(34) Berendsen, H. J. C.; van der Spoel, D.; van Drunen, R. GROMACS: A Message-Passing Parallel Molecular Dynamics Implementation. *Comput. Phys. Commun.* **1995**, *91* (1), 43–56. https://doi.org/10.1016/0010-4655(95)00042-E.

(35) Abraham, M. J.; Murtola, T.; Schulz, R.; Páll, S.; Smith, J. C.; Hess, B.; Lindahl, E. GROMACS: High Performance Molecular Simulations through Multi-Level Parallelism from Laptops to Supercomputers. *SoftwareX* **2015**, *1–2*, 19–25. https://doi.org/10.1016/j.softx.2015.06.001.

(36) Szilárd, P.; Abraham, M. J.; Kutzner, C.; Hess, B.; Lindahl, E. Tackling Exascale Software Challenges in Molecular Dynamics Simulations with GROMACS; 2015; Vol. 8759, pp 3–27. https://doi.org/10.1007/978-3-319-15976-8_1.

(37) Pronk, S.; Páll, S.; Schulz, R.; Larsson, P.; Bjelkmar, P.; Apostolov, R.; Shirts, M. R.; Smith, J. C.; Kasson, P. M.; van der Spoel, D.; Hess, B.; Lindahl, E. GROMACS 4.5: A High-Throughput and Highly Parallel Open Source Molecular Simulation Toolkit. *Bioinformatics* **2013**, *29* (7), 845–854. https://doi.org/10.1093/bioinformatics/btt055.

(38) Essmann, U.; Perera, L.; Berkowitz, M. L.; Darden, T.; Lee, H.; Pedersen, L. G. A Smooth Particle Mesh Ewald Method. *J. Chem. Phys.* **1995**, *103* (19), 8577–8593. https://doi.org/10.1063/1.470117.

(39) Miyamoto, S.; Kollman, P. A. Settle: An Analytical Version of the SHAKE and RATTLE Algorithm for Rigid Water Models. *J. Comput. Chem.* **1992**, *13* (8), 952–962. https://doi.org/10.1002/jcc.540130805.

(40) Robustelli, P.; Piana, S.; Shaw, D. E. Developing a Molecular Dynamics Force Field for Both Folded and Disordered Protein States. *Proc. Natl. Acad. Sci.* **2018**, *115* (21). https://doi.org/10.1073/pnas.1800690115.

(41) Roeters, S. J.; van Dijk, C. N.; Torres-Knoop, A.; Backus, E. H. G.; Campen, R. K.; Bonn, M.; Woutersen, S. Determining In Situ Protein Conformation and Orientation from the Amide-I Sum-Frequency Generation Spectrum: Theory and Experiment. *J. Phys. Chem. A* **2013**, *117* (29), 6311–6322. https://doi.org/10.1021/jp401159r.

(42) Lu, H.; Schäfer, A.; Lutz, H.; Roeters, S. J.; Lieberwirth, I.; Muñoz-Espí, R.; Hood, M. A.; Bonn, M.; Weidner, T. Peptide-Controlled Assembly of Macroscopic Calcium Oxalate Nanosheets. *J. Phys. Chem. Lett.* **2019**, *10* (9), 2170–2174. https://doi.org/10.1021/acs.jpclett.9b00684.

(43) Ham, S.; Kim, J.-H.; Lee, H.; Cho, M. Correlation between Electronic and Molecular Structure Distortions and Vibrational Properties. II. Amide I Modes of NMA–ND2O Complexes. *J. Chem. Phys.* **2003**, *118* (8), 3491–3498. https://doi.org/10.1063/1.1536980.

(44) Krimm, S.; Bandekar, J. Vibrational Spectroscopy and Conformation of Peptides, Polypeptides, and Proteins. *Adv. Protein Chem.* **1986**, *38*, 181–364. https://doi.org/10.1016/S0065-3233(08)60528-8.

(45) Gorbunov, R. D.; Kosov, D. S.; Stock, G. Ab Initio-Based Exciton Model of Amide I Vibrations in Peptides: Definition, Conformational Dependence, and Transferability. *J. Chem. Phys.* **2005**, *122* (22), 224904. https://doi.org/10.1063/1.1898215.

(46) Hamm, P.; Zanni, M. *Concepts and Methods of 2D Infrared Spectroscopy*; Cambridge University Press, 2011.

(47) Schmüser, L.; Trefz, M.; Roeters, S. J.; Beckner, W.; Pfaendtner, J.; Otzen, D.; Woutersen, S.; Bonn, M.; Schneider, D.; Weidner, T. Membrane Structure of Aquaporin Observed with Combined Experimental and Theoretical Sum Frequency Generation Spectroscopy. *Langmuir* **2021**, *37* (45), 13452–13459. https://doi.org/10.1021/acs.langmuir.1c02206.

(48) Lutz, H.; Jaeger, V.; Schmüser, L.; Bonn, M.; Pfaendtner, J.; Weidner, T. The Structure of the Diatom Silaffin Peptide R5 within Freestanding Two-Dimensional Biosilica Sheets. *Angew. Chem. Int. Ed.* **2017**, *56* (28), 8277–8280. https://doi.org/10.1002/anie.201702707.

(49) Miraglia, F.; Ricci, A.; Rota, L.; Colla, E. Subcellular Localization of Alpha-Synuclein Aggregates and Their Interaction with Membranes. *Neural Regen. Res.* **2018**, *13* (7), 1136–1144. https://doi.org/10.4103/1673-5374.235013.

(50) Ghosh, D.; Singh, P. K.; Sahay, S.; Jha, N. N.; Jacob, R. S.; Sen, S.; Kumar, A.; Riek, R.; Maji, S. K. Structure Based Aggregation Studies Reveal the Presence of Helix-Rich Intermediate during α-Synuclein Aggregation. *Sci. Rep.* **2015**, *5* (1), 9228. https://doi.org/10.1038/srep09228.

(51) Anderson, V. L.; Ramlall, T. F.; Rospigliosi, C. C.; Webb, W. W.; Eliezer, D. Identification of a Helical Intermediate in Trifluoroethanol-Induced Alpha-Synuclein Aggregation. *Proc. Natl. Acad. Sci.* **2010**, *107* (44), 18850–18855. https://doi.org/10.1073/pnas.1012336107.